ACS Partner Journal

Journal of the American Society for Mass Spectrometry

pubs.acs.org/jasms

Research Article

Multi-CRAFTI: Relative Collision Cross Sections from Fourier Transform Ion Cyclotron Resonance Mass Spectrometric Line Width Measurements

Brigham L. Pope, Daniel Joaquin, Jacob T. Hickey, Noah Mismash, Tina Heravi, Jamir Shrestha, Andrew J. Arslanian, Anupriya, Daniel N. Mortensen, and David V. Dearden*

Cite This: *J. Am. Soc. Mass Spectrom.* 2022, 33, 131−140

Read Online

ACCESS | Metrics & More | Article Recommendations | Supporting Information

ABSTRACT: Determination of collision cross sections (CCS) using the cross-sectional areas by the Fourier transform ion cyclotron resonance (CRAFTI) technique is limited by the requirement that accurate pressures in the trapping cell of the mass spectrometer must be known. Experiments must also be performed in the energetic hard-sphere regime such that ions decohere after single collisions with neutrals; this limits application to ions that are not much more massive than the neutrals. To mitigate these problems, we have resonantly excited two (or more) ions of different m/z to the same center-of-mass kinetic energy in a single experiment, subjecting them to identical neutral pressures. We term this approach "multi-CRAFTI". This facilitates measurement of relative CCS without requiring knowledge of the pressure and enables determination of absolute CCS using internal standards. Experiments with tetraalkylammonium ions yield CCS in reasonable agreement with the one-ion-at-a-time CRAFTI approach and with ion mobility spectrometry (IMS) when differences in collision energetics are taken into account (multi-CRAFTI generally yields smaller CCS than does IMS due to the higher collision energies employed in multi-CRAFTI). Comparison of multi-CRAFTI and IMS results with CCS calculated from structures computed at the M06-2X/6-31+G* level of theory using projection approximation or trajectory method values, respectively, indicates that the computed structures have CCS increasingly smaller than the experimental CCS as m/z increases, implying the computational model overestimates interactions between the alkyl arms. For ions that undergo similar collisional decoherence processes, relative CCS reach constant values at lower collision energies than do absolute CCS values, suggesting a means of increasing the accessible upper m/z limit by employing multi-CRAFTI.

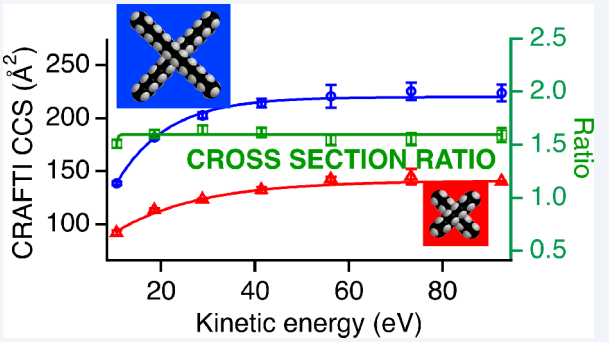

INTRODUCTION

Ion-neutral collision cross section measurements have recently increased in popularity and importance.[1−3] Measured cross sections reflect the rotationally averaged sum of the radii of the analyte ion and neutral collision gas molecule. An accurate cross section can reveal important structural information, including ligation,[1] tertiary structure,[1,2] and structural isomers.[4,5]

The current "gold standard" for measuring cross sections is ion mobility spectrometry (IMS).[1,6] Three main types of ion mobility instruments are in common use: drift tube IMS (DTIMS), traveling wave IMS (TWIMS), and field asymmetric IMS (FAIMS). In DTIMS measurements, ions are drawn by an electric field through a drift tube containing a neutral gas. The time required for the ions to traverse the drift tube is dependent on the momentum transfer cross section for collisions with the neutral (larger cross sections result in colliding more frequently with the drift gas, resulting in a slower drift). DTIMS has long served as the standard for experimentally measuring collision cross sections and for developing models to compute them.[1] TWIMS utilizes multiple ring electrodes to create a potential wave that travels down the drift tube. This traveling potential wave pushes the ions forward, while collisions with the background gas retard their motion; the balance between these forward and retarding forces enables the cross section measurement. While FAIMS does separate ions based on differences in mobility and how these differences change with changes in the electric field, FAIMS results are more difficult to convert into collision cross sections,[7] and to our knowledge this has not yet been done.

Collision cross section measurements obtained by IMS techniques have been shown to be fast, accurate, and precise.

Received: September 21, 2021
Revised: December 2, 2021
Accepted: December 7, 2021
Published: December 20, 2021

https://doi.org/10.1021/jasms.1c00297
J. Am. Soc. Mass Spectrom. 2022, 33, 131−140

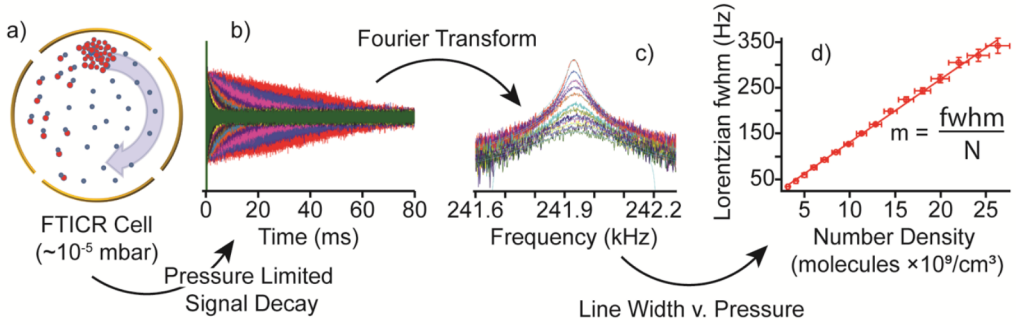

Figure 1. Schematic depiction of the CRAFTI method. (a) Ions collide with Ar background gas in the FTICR cell, (b) resulting in a transient signal decay that is dependent on the ion-neutral collision rate, which in turn is dependent on the pressure. Different traces represent different pressures, with the highest pressures (green trace) giving the fastest signal decay. (c) Peaks in the mass spectra resulting from Fourier transform of the transients are fit with a Lorentzian function. The highest pressures yield the broadest peaks. (d) The Lorentzian full-width at half-maximum line widths (fwhm) increase linearly with the neutral collision gas number density (N).

However, despite their many strengths, IMS measurements have some limitations. Perhaps the most notable limitation arises from the ion heating that can occur as the ion moves along the drift tube.[1] As a result of the multiple low-energy collisions that are inherent to drift IMS, weakly bound complexes may unfold and/or dissociate.[8]

Low energy ion-neutral collisions involve momentum transfer through long-range interactions, such as charge-induced dipole interactions, that can complicate modeling and interpretation of the results.[9,10] Experimental collision cross sections are often compared with values computed from proposed molecular structures, usually with the goal of determining which structures are plausible. Accurate cross section calculations require some knowledge of long-range ion−molecule interaction potentials to obtain optimum agreement with ion mobility-based experiments, and computational approaches that produce excellent agreement with DTIMS results have been developed.[11,12]

Another complementary approach to collision cross section measurement has recently been described.[13−15] CRAFTI is an acronym for *c*ross sectional *a*reas by *F*ourier *t*ransform *i*on cyclotron resonance mass spectrometry (FTICR-MS). In FTICR experiments, ions in a magnetic field are detected using the image charge that groups of coherently orbiting ions induce in the detection electrodes. Coherent motion of the ion packet is brought about through the application of a radio frequency (RF) electric field that causes the ions to accelerate and phase align with the RF field. This state of coherent motion decays over time after the RF field is turned off. At sufficiently high background gas pressures, the primary cause of decay is collisions with the background gas. These collisions may scatter the ions out of coherent motion through momentum transfer or may cause collision-induced dissociation (which changes the mass-to-charge ratio and the cyclotron frequency of the ions, removing them from the coherently orbiting packet of ions). The collision rate depends on the ion velocity, on the neutral background gas pressure, and on the collision cross section. The ion velocity is easily determined from the known ion excitation parameters, so if the neutral pressure is known and the decoherence rate is measured, the collision cross section can be determined (see Figure 1). A key assumption of the method is that every ion-neutral collision removes the ion from the coherent group (i.e., we assume single-collision decoherence). The decoherence rate can be determined either by analyzing the signal decay in the time domain[16−18] or by using a Fourier transform to convert to the frequency domain and measuring the width of the power spectral peak.[13−15] Because the frequency domain spectrum is routinely determined in obtaining the mass spectrum, we have taken the latter approach. Plots of peak width as a function of the pressure inside the cell exhibit a linear relationship under single-collision decoherence conditions.[15] CRAFTI has already been shown to give collision cross sections that are consistent with IMS measurements and computational methods for the protonated ions of the 20 biological amino acids and for crown ether−ammonium complexes.[14,15]

CRAFTI has several attractive features. First, CRAFTI can be performed on any Fourier transform-based mass analyzer without expensive modifications. We[13−15] and others[16−18] have implemented CRAFTI using FTICR/MS. Sanders et al. reported cross section measurements from the decay of coherent motion in their orbitrap instrument.[19] This approach is similar in concept to CRAFTI but differs in that coherent motion is induced in the orbitrap by injecting all the ions as a packet rather than by using resonant excitation; signal is monitored as ions move as a group between the two halves of the trap and coherent motion decays as a result of collisions with residual nitrogen. As a result, independent control of the collision energies of ions of different m/z is not currently available. Results are extracted by Fourier filtering to determine signal decay rates and corresponding collision cross sections. The method is quite promising because it works at very low pressures, preserving the excellent mass resolving power of the instrument, and has been successfully applied for protein ions.

In another application of the concept of measuring collision cross sections by measuring ion cloud decoherence, Dziekonski et al.[20,21] and Elliot et al.[22] presented cross section measurements taken using an electrostatic ion trap employing charge detection, a process Dziekonski et al. termed "CRAFTI-EST".[20]

CRAFTI measures cross section using mass spectrometric line widths, which are already routinely measured. Hence, the analyst can potentially find both the collision cross section and the mass-to-charge ratio using a single measurement in a single instrument. This ability to perform cross section measurements with an existing instrument is what motivated our initial interest in CRAFTI.

Because CRAFTI is a single-collision technique, fragile molecules that cannot survive the multiple collision environment of a drift tube can be measured.[23] Further, the kinetic

https://doi.org/10.1021/jasms.1c00297
J. Am. Soc. Mass Spectrom. 2022, 33, 131−140

energies of ions accelerated into coherent motion in an FTICR or orbitrap experiment are typically at least tens of eV in the center-of-mass frame of reference (limited by the orbit radius that allows the ions to remain within the trap and the relative masses of the ion and neutral), so collisions can generally be described using simple hard-sphere models that do not require consideration of more complex, long-range ion-neutral interaction potentials.[9,10]

While CRAFTI shows promise, it still has some significant limitations. First, accurate CRAFTI measurements require accurate pressures measured in the trapping cell, which can be difficult to obtain. Most pressure measurements require a separate transducer (such as a cold cathode tube, for example), and most such transducers do not function well in a high magnetic field so they have to be placed at some distance from the trapping cell. It is possible to obtain pressures in the trapping cell by using ion−molecule reaction kinetics when rate constants are known[24,25] or line width measurements when accurate energy-dependent collision cross sections are known,[26] but only a limited number of systems are available that can be used. Any error in pressure measurement will have corresponding effects on the resulting cross section measurement.

More seriously, the single-collision decoherence requirement means CRAFTI measurements have a fairly low upper m/z limit because ions of large m/z, even in large orbits, have low center-of-mass kinetic energies such that single-collision decoherence cannot be assumed. This makes it challenging to apply CRAFTI to larger biomolecules. We can mitigate these limitations by measuring two or more ions at the same time under identical pressure conditions with center-of-mass reference frame kinetic energies that are the same to within a fraction of 1 eV. This paper presents a multiple ion CRAFTI technique ("multi-CRAFTI") and compares its results with results from single ion CRAFTI, IMS, and computed cross section values.

EXPERIMENTAL SECTION

Mass spectra were acquired using a Bruker APEX 47e Fourier transform ion cyclotron resonance mass spectrometer controlled with a MIDAS Predator data system (National High Magnetic Field Laboratory, Tallahassee, FL).[27] The mass spectrometer is equipped with a 4.7 T magnet, an Infinity trapping cell,[28,29] a microelectrospray source modified from a design by Analytica (Branford, CT), and a metal capillary drying tube based on a design by Eyler.[30] Stored waveform inverse Fourier transform techniques were used to isolate monoisotopic ions of interest.[31] Mass spectra were analyzed using the Igor Pro software package (version 7, Wavemetrics, Lake Oswego, OR).

Argon collision gas was introduced using a Freiser-type pulsed leak valve,[32] and the steady-state pressure was varied by varying the time the solenoid valve that pressurized the leak was open. Accurate pressure measurements were obtained using the line width pressure measurement technique we refer to as "LIPS", which is described in detail elsewhere.[26] Briefly, LIPS measures Ar^+ frequency-domain line widths (and, hence, collision frequencies) in neutral Ar over a series of pulsed-leak valve times using Ar^+ ions created through in-cell electron impact ionization. The literature collision cross section of Ar^+ in Ar at the experimental kinetic energy (as determined by Phelps et al.)[33] is then used to calculate the background collision gas number density, N, from the measured full-width at half-maximum (fwhm) line widths in the mass spectra using the CRAFTI equation:[15]

$$\sigma = \frac{\text{fwhm}}{N}\frac{m}{q}\frac{\pi d}{\beta V_{\text{PP}} T_{\text{exc}}} \quad (1)$$

Here, σ is the collision cross section, m and q are the ion mass and charge, respectively, d is the cell diameter (0.06 m), β is the cell geometry factor (0.897 for the Infinity trapping cell used here), V_{PP} is the peak-to-peak excitation voltage, and T_{exc} is the excitation duration. The fwhm line widths are obtained using Lorentzian fits to the mass spectral data (Figure 1c). Pressurization solenoid valve times of 10−160 ms were used, resulting in number densities of between about 3×10^9 and 27×10^9 molecules cm^{-3} (Figure 1d).

In single-ion CRAFTI experiments, the ion of interest was excited on resonance for 450 μs in the presence of Ar background gas using excitation voltages of 1−35 V. In all experiments, care was taken to avoid approaching the space charge limit of our trapping cell. This was done by monitoring the shape of the transient signal and that of the resulting spectral lines to ensure they retain Lorentzian shapes, adjusting signal level as needed to maintain Lorentzian lines. Standard practice was to use the slope obtained from a plot of the fwhm line widths as a function of background gas number density as the first term in eq 1 (fwhm/N). In multi-CRAFTI experiments, the excitation waveform was generated by phase-continuous concatenation of two single-frequency sinusoidal excitation waveforms using a LabVIEW (National Instruments; Austin, TX; 2016 version) program. The two ions were, therefore, sequentially excited at their resonant frequencies, the heavier ion (lower resonant frequency) first and the lighter ion (higher frequency) second. The durations of the low- and high-frequency portions of the excitation waveform were adjusted so that both ions achieved the same kinetic energy in the center-of-mass reference frame to within experimental error. The postexcitation center-of-mass kinetic energy (KE) was determined using the equation[34]

$$\text{KE} = \frac{1.20607 \times 10^7 z^2 V_{\text{PP}}^2 T_{\text{exc}}^2}{d^2 m_{\text{ion}}}\frac{m_{\text{neutral}}}{m_{\text{neutral}} + m_{\text{ion}}} \quad (2)$$

Here, z is the ion charge in multiples of the fundamental charge, and m_{ion} and m_{neutral} are the masses of the ion and neutral background gas, respectively. The heavier ion was excited for 450 μs, and the excitation time for the lighter ion was determined by solving eq 2 for T_{exc} using the kinetic energy value determined for the heavier ion. For a constant KE, T_{exc} is proportional to the square root of the mass of the ion and thus decreases with decreasing mass. Therefore, the excitation time for the lighter ion was always less than that for the heavier ion. All kinetic energies reported herein are in the center-of-mass reference frame.

For multi-CRAFTI experiments, the ratio of cross sections of the two ions (denoted σ_1/σ_2) was determined by writing eq 1 for each ion and taking the ratio for the two ions:

$$\frac{\sigma_1}{\sigma_2} = \frac{\text{fwhm}_1}{\text{fwhm}_2}\frac{m_1 q_2}{m_2 q_1}\frac{V_{\text{PP},2} T_{\text{exc},2}}{V_{\text{PP},1} T_{\text{exc},1}} \quad (3)$$

This affords cancellation of many of the terms in eq 1, notably including the neutral number density (because both ions experience the same neutral collision gas pressure). Additionally, in the current study, the same excitation voltage was used

https://doi.org/10.1021/jasms.1c00297
J. Am. Soc. Mass Spectrom. 2022, 33, 131−140

for both ions, allowing the terms $V_{PP,2}$ and $V_{PP,1}$ to cancel. Similarly, eq 3 does not depend on the magnetic field strength or cell geometry. Uncertainties reported for both the single-ion and multi-CRAFTI methods of determining CRAFTI cross sections are standard errors obtained from Lorentzian fits to obtain the line widths, propagated through repeated measurements.

Computationally, conformational searches were performed for ions of interest using the Spartan '16 package (Wave function, Inc., Irvine, CA) with the included Merck Molecular Force Field (MMFF94).[35−39] Low energy structures from the conformational searches were further refined by full geometry optimization at the M06-2X/6-31+G* level of theory. The resulting structures were then input into the IMoS[12] software package (version 1.10c) to compute projection-approximation collision cross sections using Ar as the collision gas. Boltzmann-weighted average collision cross sections were then determined using the relative energies of the different conformers to determine the Boltzmann distribution. Uncertainties reported for IMoS cross sections are the standard deviations resulting from the Boltzmann-weighted averaging. We also used IMoS to calculate cross sections for comparison with IMS experiments. In these cases, to match the IMS experiments we used N_2 as the collision gas (with its quadrupole moment considered) and included ESP partial charges from the ab initio calculations.

Cryptand [2.2.2], 2-propanol, and bromide salts of tetraethylammonium, tetrabutylammonium, tetraoctylammonium, tetradodecylammonium, and tetrahexadecylammonium were obtained from Sigma-Aldrich (St. Louis, MO). For convenience in referring to the tetraalkylammonium species, the shorthand NCX^+, where X = the number of carbons in a single alkyl chain, is used. Analytes were dissolved at a concentration of ∼100 μM in a 50:50 water/2-propanol mixture for electrospray ionization.

RESULTS

Single-Ion CRAFTI Experiments. Collision cross sections obtained for NC2$^+$, NC4$^+$, NC8$^+$, NC12$^+$, and NC16$^+$ using the single-ion CRAFTI method are shown in Figure 2a as a function of kinetic energy. For most of the ions shown here (and for most others we have observed[40]), the collision cross section increases with increasing kinetic energy until an asymptotic value is reached. In general, cross sections at low kinetic energies tend to be inaccurate because single-collision decoherence is not achieved and signal is poor with insufficient excitation. We believe this accounts for the anomalous points at low collision energies observed for NC2$^+$. Theory suggests that CCS should decrease at high collision energies, but at the energies accessible in most of our experiments this is a change that is too small for our methods to observe. At the highest kinetic energies problems arise because ions are ejected from the trapping cell, again resulting in loss of signal. For NC12$^+$ and NC16$^+$ an asymptotic value is not fully achieved at energies that are experimentally accessible.

When sufficiently energetic collisions are possible, the asymptotic CCS values of the tetraalkylammonium ions can be obtained by fitting the data such as that in Figure 2a with an exponential function of the form:

$$f(\mathrm{KE}) = \sigma_{\mathrm{hs}} - Ae^{-\left(\frac{\mathrm{KE}}{\tau}\right)} \quad (4)$$

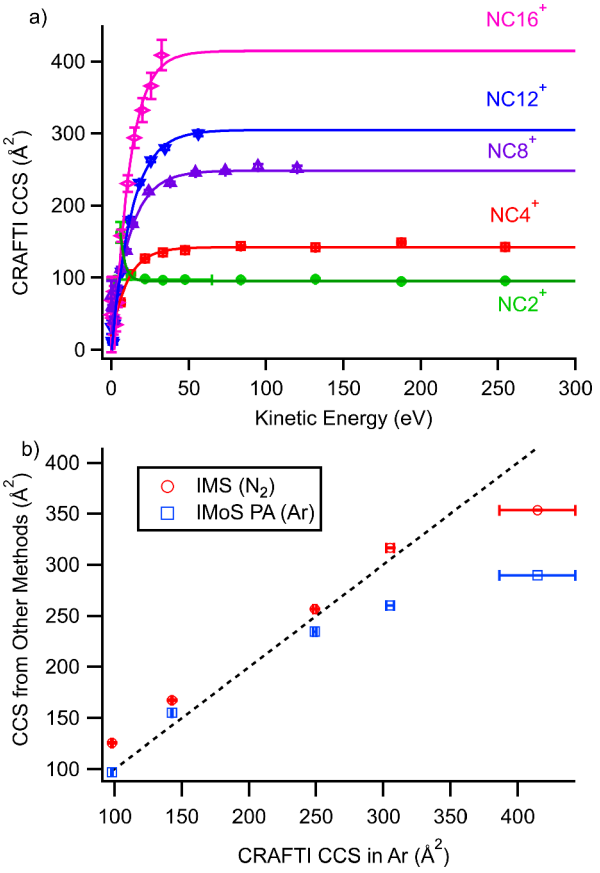

Figure 2. (a) Single-ion method CRAFTI cross sections obtained for NC2$^+$ (green diamonds), NC4$^+$ (red squares), NC8$^+$ (purple triangles), NC12$^+$ (blue triangles), and NC16$^+$ (magenta diamonds) as a function of kinetic energy. Solid lines are exponential fits to the data. (b) Cross sections of the various alkylammonium ions measured previously using IMS (red circles) and computed using IMoS projection approximation (blue squares) relative to the corresponding CRAFTI cross sections. The dashed black line indicates a 1:1 correlation between the axes.

Here, A and τ are positive scaling factors and σ_{hs} corresponds to the hard sphere CCS. Cross sections measured using IMS and computed from theoretical structures using the IMoS projection approximation are plotted relative to the corresponding measured CRAFTI cross sections in Figure 2b. Reasonable agreement is generally observed, but poor agreement is seen for the NC16$^+$ ion, wherein the CRAFTI cross section is about 17% larger than that obtained using IMS and about 43% larger than that obtained using the IMoS projection approximation for model structures. This is not surprising given that an asymptotic CCS value was not observed for this ion in the CRAFTI experiments, so the asymptote of the exponential fit is strongly dependent on a few points at the highest energies. Therefore, CRAFTI experiments for NC16$^+$ are not expected to be accurate.

Multi-CRAFTI Experiments. Multi-CRAFTI experiments were performed by sequentially exciting various pairs of alkylammonium cations. A representative plot of the ratio of cross sections obtained using the multi-CRAFTI method for σ(NC12$^+$)/σ(NC8$^+$) is shown in Figure 3 as a function of kinetic energy. Also shown in Figure 3 are the relative single-ion CRAFTI cross sections obtained for NC8$^+$ and NC12$^+$ in this same set of experimental acquisitions (accurate pressures

https://doi.org/10.1021/jasms.1c00297
J. Am. Soc. Mass Spectrom. 2022, 33, 131−140

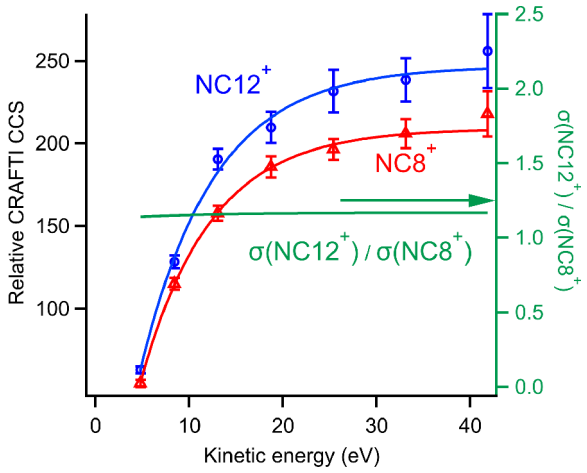

Figure 3. Cross sections obtained for $NC8^+$ (red triangles) and $NC12^+$ (blue circles) using multi-CRAFTI excitation (left axis) and the ratio of cross sections for these ions (right axis, green curve) as a function of kinetic energy. Arrows indicate the relevant axes. Solid lines are exponential fits to the data.

in the trapping cell were not measured, so the absolute collision cross section values are not accurate). The ratio of cross sections obtained using the multi-CRAFTI method increases with increasing kinetic energy until an asymptotic value is achieved, similar to what is observed with the single-ion method.[40] However, here we are looking at ratios rather than absolute cross sections. Interestingly, the ratio of cross sections for $NC8^+$ and $NC12^+$ reaches an asymptotic value (it is nearly constant over the range measured here) at a significantly lower kinetic energy (~10 eV) than is required to reach an asymptotic value for either ion alone (~40 eV or more, where it could be argued $NC12^+$ does not actually achieve the asymptotic value).

The high-energy limiting ratio of collision cross sections with Ar gas (σ_1/σ_2) is obtained from the multi-CRAFTI results by fitting the ratio data as a function of kinetic energy (KE) with an exponential equation analogous to eq 4, where again A and τ are positive fitting parameters:

$$f(\mathrm{KE}) = \frac{\sigma_1}{\sigma_2} - Ae^{-\left(\frac{\mathrm{KE}}{\tau}\right)} \quad (5)$$

High-energy limit ratio values determined in this way for tetraalkylammonium cations relative to tetraoctylammonium are compiled in Table 1, along with similar ratios computed using the projection approximation in Ar and from IMS measurements in N_2 (both from the literature[41] and from our lab) and using trajectory method calculations, also in N_2.

The choice of tetraoctylammonium ion as a reference ion in Table 1 was arbitrary. We also used other pairings to make relative measurements; these can be compared by using the projection approximation collision cross sections in Ar as standards to calculate absolute collision cross sections for the various analyte ions in Ar. The results of these comparisons are shown in Table 2, which lists the ions chosen as references in each experiment in the left-hand column. Projection approximation collision cross sections in Ar from IMoS calculations on full geometry-optimized M06-2X/6-31+G* structures were assumed correct for each reference ion and used with multi-CRAFTI collision cross section ratios to calculate the values in each column, such that looking down a given column one can compare the values obtained for a given ion using different reference ions. Uncertainties are from uncertainties in the measured ratios. Agreement between IMoS projection approximation and measured multi-CRAFTI cross sections is within experimental uncertainties except for the heavier ions, $NC12^+$ and $NC16^+$, for which the experimental results are higher than the calculated values. For each ion examined, cross sections determined in this way decrease as the reference ion m/z increases.

Cryptand [2.2.2]. The multi-CRAFTI method was also used to measure the previously unreported cross section of protonated cryptand $[2.2.2]H^+$ ($C_{18}H_{36}N_2O_6H^+$, skeletal structure shown in Figure 4), a member of the cryptand family of chelating agents.[42,43] The CRAFTI cross section of $[2.2.2]H^+$ was measured using $NC4^+$, $NC8^+$, $NC12^+$, and $NC16^+$ and their corresponding projection approximation cross sections in Ar as reference values. A representative plot of the ratio of cross sections obtained using $NC12^+$ as the reference ion is shown in Figure 4 as a function of kinetic energy. The cross section for $[2.2.2]H^+$ appears to reach an asymptotic value at center-of-mass collision energies of 40 eV or less. Values of 154.9 ± 1.7, 150.7 ± 1.5, 144.2 ± 2.7, and 143.6 ± 19.2 Å^2 were obtained when $NC4^+$, $NC8^+$, $NC12^+$, and $NC16^+$ were used as references, respectively. All of these values are in generally good agreement, and again, the values decrease as m/z for the reference ion increases. The calculated cross section of $[2.2.2]H^+$ obtained using IMoS is 151.4 ± 0.1 Å^2, which is also in good agreement with the experimentally determined values.

DISCUSSION

CRAFTI Experiments on Tetraalkylammonium Ions. As we have previously noted,[40] CRAFTI collision cross sections for most ions increase with increasing collision energy, reaching an asymptotic value when decoherence occurs on every collision. This corresponds to the energetic hard sphere collision conditions described previously.[16−18,44,45] For

Table 1. Collision Cross Sections of Selected Tetraalkylammonium (NCx^+) Cations Relative to that of Tetraoctylammonium ($NC8^+$)

		$\sigma(NCx^+)/\sigma(NC8^+)$				
ion	MW (Da)	multi-CRAFTI	IMoS PA (Ar)[a]	IMS (N_2)[41]	IMS (N_2)[b]	IMoS TM (N_2)[c]
$NC2^+$	130.25	0.33 ± 0.01	0.41	0.476	0.490 ± 0.002	0.472
$NC4^+$	242.46	0.63 ± 0.01	0.66	0.649	0.652 ± 0.002	0.687
$NC12^+$	691.32	1.17 ± 0.03	1.11	1.243	1.233 ± 0.002	1.147
$NC16^+$	915.04	1.41 ± 0.03	1.24	1.409	1.377 ± 0.002	1.285

[a]Computed using IMoS projection approximation in argon. [b]This work. [c]Computed using the IMoS trajectory method in N_2 with a Lennard-Jones 4−6−12 potential, ESP charge distribution on the ion, and with N_2 quadrupole potential included

https://doi.org/10.1021/jasms.1c00297
J. Am. Soc. Mass Spectrom. 2022, 33, 131−140

Table 2. Collision Cross Sections in Ar from Multi-CRAFTI Measurements against Various Reference Ions

	collision cross section in Ar (Å^2)				
	$NC2^+$	$NC4^+$	$NC8^+$	$NC12^+$	$NC16^+$
IMoS PA (Ar)	97	155	235	260	290
reference ion					
$NC2^+$		182 ± 16	306 ± 23		
$NC4^+$	94 ± 8		262 ± 04	336 ± 6	
$NC8^+$	84 ± 6	143 ± 2		302 ± 5	420 ± 10
$NC12^+$		128 ± 3	213 ± 04		
$NC16^+$			194 ± 03		
average	89 ± 10	151 ± 28	252 ± 41	319 ± 24	420 ± 10

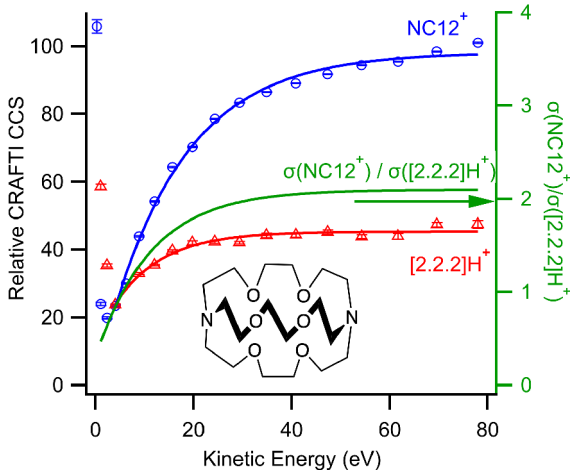

Figure 4. Relative collision cross sections in Ar obtained for $NC12^+$ (blue circles) and cryptand $[2.2.2]H^+$ (red triangles) using multi-CRAFTI excitation (left axis) and the ratio of cross sections of these ions (right axis, green curve) as a function of kinetic energy. Solid lines are exponential fits to the data, ignoring a few points at low kinetic energies that clearly do not fit the exponential trend. The structure of [2.2.2] is inset.

the tetraalkylammonium cations examined here, center-of-mass frame kinetic energies of 40−50 eV are required to reach the asymptotic limit (Figure 2). This presents a significant problem when the analyte ions are much more massive than the neutral collision gas because cyclotron orbit radii corresponding to the required energies are larger than the FTICR trapping cell; we appear to reach this condition in these experiments for $NC12^+$, m/z 691, and $NC16^+$, m/z 915, is definitely heavy enough that the asymptotic limit is not reached. This requirement limits the application of single-ion CRAFTI to low values of m/z, but this could be mitigated by examining weakly bound ions, which dissociate (and therefore decohere) at low collision energies, or of course by the expensive route of using a higher magnetic field. An additional approach, based on multi-CRAFTI, is discussed below.

When the conditions of single-collision decoherence and accurately measured neutral collision gas pressure are met, the results of CRAFTI experiments agree well with collision cross sections calculated for model structures using the simple projection approximation method and also correlate well with cross sections derived from ion mobility measurements.[15] Low-energy dissociation of the tetraalkylammonium ions does not appear to perturb the results. Interestingly, the values from CRAFTI are smaller than those from IMS (the points comparing CRAFTI with IMS fall above the 1:1 correlation line in Figure 2b) except in the case of $NC16^+$ (which, as described above, is not measured accurately), perhaps reflecting the fact that IMS includes greater contributions from long-range interactions than does CRAFTI. The importance of long-range interactions is strongly velocity-dependent (and therefore energy-dependent).[10] IMS experiments are conducted at essentially thermal energies (a fraction of 1 eV), whereas CRAFTI collision energies are typically tens to hundreds of eV.

Evaluation of the Multi-CRAFTI Method. Multi-CRAFTI, as described here, directly compares the collision cross sections of two ions under identical pressure conditions, with the same center-of-mass collision energies, so it produces ratios of collision cross sections rather than absolute values. Absolute values for analyte ions can of course be obtained from multi-CRAFTI if the pressure and excitation amplitudes are accurately known. In many experiments, relative values are sufficient, with the large advantage that knowledge of the neutral collision gas pressure is not needed. For example, host−guest complexes can be compared with a reference host ion of known structure to determine whether the guest is bound inside a host's binding site or on the exterior of the host.[23]

If absolute collision cross sections are desired, a route that avoids the need for accurate pressure measurements is to derive the absolute cross section from the cross section ratios when an accurate collision cross section for a reference ion is known. This is the approach we took in Table 2, relying on computed structures to provide the reference collision cross sections. Obviously, the accuracy of this approach depends on having accurate reference values, and perusal of Table 2, as well as the values obtained for $[2.2.2]H^+$, indicates a potential problem.

It is interesting to note that both the multi-CRAFTI measurements reported here and the IMS results (both ours and those reported previously,[41] which are in good agreement) compiled in Table 2 suggest flaws in the model structures we obtained for the tetraalkylammonium cations. This can perhaps be seen most easily by plotting CRAFTI collision cross sections against projection approximation cross sections computed from model structures, which were obtained from full geometry optimization at the M06-2X/6-31+G* level of theory, and by plotting IMS collision cross sections against trajectory method values from the same model structures (Figure 5).

The plot shows that experimental ratios increase faster with m/z than the best available computed ratios increase, for both multi-CRAFTI and IMS measurements (the slopes of the linear fits to each data set are greater than 1). One plausible explanation is that intramolecular interactions between the alkyl arms of the ions are overestimated in the model

https://doi.org/10.1021/jasms.1c00297
J. Am. Soc. Mass Spectrom. 2022, 33, 131−140

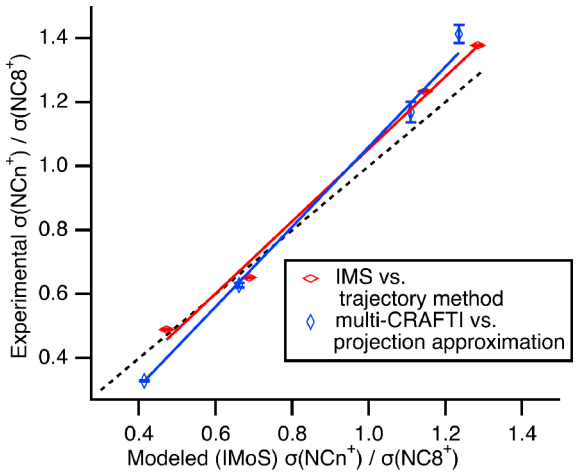

Figure 5. Experimentally measured collision cross sections relative to that of tetraoctylammonium ($NC8^+$) for IMS (red) and multi-CRAFTI (blue) as a function of the corresponding computed collision cross section ratios determined using the trajectory method (in the case of IMS) or using the projection approximation (in the case of multi-CRAFTI). Solid lines are linear least-squares fits to each data set, and the dotted line represents the exact 1:1 agreement between experimental and computed values.

structures, making the model structures more compact than they should be. This would become increasingly problematic as m/z increases and intramolecular interactions increase. Such overestimation would not be surprising because weak noncovalent interactions are difficult to model accurately and it is certain that the ions are vibrationally hotter than the 0 K structures of the models. If this is the case, this could explain why the collision cross section values derived from the multi-CRAFTI ratios, both for the values in Table 2 and for $[2.2.2]H^+$, become increasingly smaller as m/z for the reference ion increases.

The need for appropriate internal standards is highlighted by a multi-CRAFTI experiment comparing $NC8^+$ with Cs^+ (Figure 6). The apparent cross section for $NC8^+$, which decoheres primarily by collision-induced dissociation, increases with kinetic energy and approaches a constant value around

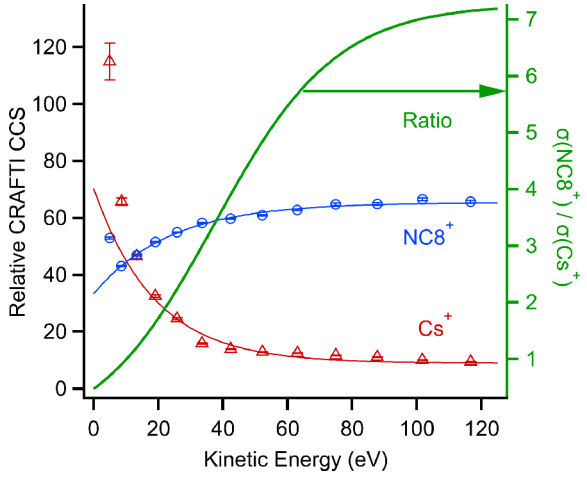

Figure 6. Cross sections obtained for $NC8^+$ (blue circles) and Cs^+ (red triangles) in Ar using multi-CRAFTI (left axis) and the ratio of cross sections of these ions (right axis, green curve) as a function of kinetic energy. Solid lines are exponential fits to the data.

50−100 eV. The measurements for Cs^+, which cannot decohere by collision-induced dissociation and therefore loses coherence primarily via momentum-transfer collisions, *decrease* with increasing collision energy as expected (because higher-energy collisions lead to greater interpenetration of the electron clouds of Cs^+ and Ar). The resulting cross section ratio plateaus at higher energies than does the collision cross section for $NC8^+$ alone, suggesting Cs^+ would be a poor internal standard in this case.

This difference in decoherence mechanisms is illustrated by additional experiments (Figure 7) that excited the ions in the

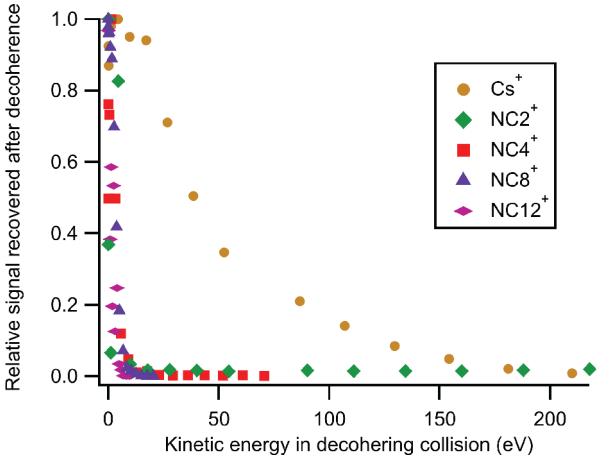

Figure 7. Relative ion population in the trap after a single-frequency excitation at the given center-of-mass kinetic energy and with Ar in the cell to cause decoherence. After complete decoherence, the remaining ions were re-excited for detection. Tetraalkylammonium ions were all lost at similar low excitation energies, indicating that the main mechanism for decohering them was collision-induced dissociation. Cs^+, on the other hand, decoheres primarily by momentum transfer collisions with Ar and remains in the trapping cell until collisions cause scattering sufficient to remove it.

same way as we normally excite them for a CRAFTI experiment with Ar collision gas present, followed by a delay to allow complete decoherence of the coherently excited ions, followed by a normal excitation-detection sequence. The objective of these experiments was to measure what fraction of the ion population remained in the trapping cell after the first decohering collision. All of the tetraalkylammonium ions examined are lost at very low decoherence collision energies as they undergo collision-induced dissociation. Cs^+, on the other hand, cannot dissociate and remains in the trapping cell following the decohering collision until much higher collision energies scatter it out of the cell.

Good internal standards in multi-CRAFTI, for which eq 3 should be valid, should have the following characteristics. If the goal is measurement of accurate absolute collision cross sections, the standard must have a well-characterized cross section. Practically speaking, excitation of standard and analyte is easier if the two have similar m/z but with cyclotron frequencies that are well enough separated that significant off-resonant excitation of one ion does not occur when exciting the other, complicating the analysis. Ideally, the reference ion should decohere by a similar mechanism to the analyte to facilitate reaching asymptotic collision cross section ratios at lower kinetic energies. If the analyte of interest is easily decohered, this requirement can probably be relaxed some-

https://doi.org/10.1021/jasms.1c00297
J. Am. Soc. Mass Spectrom. 2022, 33, 131−140

what. For example, even though the tetraalkylammonium cations used as standards all decohere primarily by collision-induced dissociation, no fragment ions of analyte $[2.2.2]H^+$ (Figure 4) were observed, suggesting either that $[2.2.2]H^+$ decoheres by some other mechanism or that the fragments were below the low-mass (high-frequency) cutoff of our instrument (about m/z 20 in these experiments). However, $[2.2.2]H^+$ does appear to reach asymptotic collision cross section values around a relatively low value of about 20 eV. The measurements yielded an average value of 148 ± 5 Å^2 for the collision cross section of this ion with Ar, in excellent agreement with the projection approximation value of 151 Å^2 for the model structure.

CONCLUSIONS

In summary, the multi-CRAFTI approach has several advantages over measuring one ion at a time while retaining the rigorous control of the excitation process that is inherent in the single-ion method. Measuring two ions at once offers a multiplex advantage. Several advantages arise from the fact that the two ions are compared simultaneously, such that conditions in the trapping cell are identical for the two ions; the fact that accurate absolute pressure measurements are therefore not needed is a large advantage. Further, multi-CRAFTI facilitates the use of reference ions of known collision cross section as internal standards. In addition, because multi-CRAFTI ratios become constant at lower kinetic energies than do absolute cross section measurements, somewhat heavier ions, which cannot be accelerated to high center-of-mass energies while remaining in the trap, can be addressed. With our 4.7 T magnet, this has currently enabled us to increase the upper m/z limit by about 30%, to approximately m/z 1300, in favorable cases involving ions that dissociate easily (doubly charged cucurbit[n]uril complexes) and using heavier collision gases (SF_6). It would of course be desirable to go to much higher m/z to enable application to interesting biomolecules, and one obvious approach would be to use higher magnetic fields because trappable kinetic energies scale with the square of the field strength. Reports of measurements at 9.4 T using methods that are very similar to CRAFTI with ions as large as ubiquitin and cytochrome c are in the literature.[17,18,45] We are currently in the process of trying multi-CRAFTI techniques at higher field.

The concept of multi-CRAFTI could easily be extended beyond just pairs of ions; we have done experiments with as many as four ions simultaneously excited and compared using single-frequency excitations. For the sake of simplicity, in the experiments described in this paper we have used single-frequency excitation, but other strategies are viable. Although the analysis is more complicated, chirp excitation could be used to compare many ions in a single experiment. Other excitation strategies could also be used. For example, we excited the ions sequentially here by concatenating single-frequency waveforms and controlling the degree of excitation by controlling the duration of each excitation component. Another approach would be to sum waveforms of each required frequency, controlling the peak-to-peak amplitudes of the various frequency components to control the degree of excitation. In the experiments described here, we chose to control the excitation to drive the ions under comparison to identical center-of-mass collision energies. However, this was an arbitrary choice, and perhaps excitation to identical velocities for all ions being compared would be better because at constant velocity any difference in collision frequency would depend only on differences in collision cross sections.

ASSOCIATED CONTENT

Supporting Information

The Supporting Information is available free of charge at https://pubs.acs.org/doi/10.1021/jasms.1c00297.

Collision-induced dissociation mass spectrum and precursor ion survival curve for tetraoctylammonium ion; comparison of collision-induced dissociation and multi-CRAFTI ratios as a function of collision energy (PDF)

AUTHOR INFORMATION

Corresponding Author

David V. Dearden − *Department of Chemistry and Biochemistry, Brigham Young University, Provo, Utah 84602-1030, United States;* orcid.org/0000-0003-0899-7776; Phone: +1 (801) 422-2355; Email: dvd@chem.byu.edu; Fax: +1 (801) 422-0153

Authors

Brigham L. Pope − *Department of Chemistry and Biochemistry, Brigham Young University, Provo, Utah 84602-1030, United States*

Daniel Joaquin − *Department of Chemistry and Biochemistry, Brigham Young University, Provo, Utah 84602-1030, United States*

Jacob T. Hickey − *Department of Chemistry and Biochemistry, Brigham Young University, Provo, Utah 84602-1030, United States*

Noah Mismash − *Department of Chemistry and Biochemistry, Brigham Young University, Provo, Utah 84602-1030, United States*

Tina Heravi − *Department of Chemistry and Biochemistry, Brigham Young University, Provo, Utah 84602-1030, United States*

Jamir Shrestha − *Department of Chemistry and Biochemistry, Brigham Young University, Provo, Utah 84602-1030, United States*

Andrew J. Arslanian − *Department of Chemistry and Biochemistry, Brigham Young University, Provo, Utah 84602-1030, United States*

Anupriya − *Department of Chemistry and Biochemistry, Brigham Young University, Provo, Utah 84602-1030, United States*

Daniel N. Mortensen − *Department of Chemistry and Biochemistry, Brigham Young University, Provo, Utah 84602-1030, United States*

Complete contact information is available at: https://pubs.acs.org/10.1021/jasms.1c00297

Author Contributions

The manuscript was written through contributions of all authors.

Notes

The authors declare no competing financial interest.

ACKNOWLEDGMENTS

The authors thank the National Science Foundation for financial support (CHE-1904838).

REFERENCES

(1) Lanucara, F.; Holman, S. W.; Gray, C. J.; Eyers, C. E. The power of ion mobility-mass spectrometry for structural characterization and the study of conformational dynamics. *Nat. Chem.* **2014**, *6*, 281−294.
(2) Tian, Y.; Ruotolo, B. T. The growing role of structural mass spectrometry in the discovery and development of therapeutic antibodies. *Analyst* **2018**, *143*, 2459−2468.
(3) Williams, D. M.; Pukala, T. L. Novel insights into protein misfolding diseases revealed by ion mobility-mass spectrometry. *Mass Spectrom. Rev.* **2013**, *32*, 169−187.
(4) Majuta, S. N.; Maleki, H.; Karanji, A. K.; Attanyake, K.; Loch, E.; Valentine, S. J. Magnifying ion mobility spectrometry-mass spectrometry measurements for biomolecular structure studies. *Curr. Opin. Chem. Biol.* **2018**, *42*, 101−110.
(5) Kanu, A. B.; Dwivedi, P.; Tam, M.; Matz, L.; Hill, H. H. Ion mobility-mass spectrometry. *J. Mass Spectrom.* **2008**, *43*, 1−22.
(6) Zhong, Y.; Hyung, S.-J.; Ruotolo, B. T. Ion mobility-mass spectrometry for structural proteomics. *Expert Rev. Proteomics* **2012**, *9*, 47−58.
(7) Dodds, J. N.; May, J. C.; McLean, J. A. Correlating Resolving Power, Resolution, and Collision Cross Section: Unifying Cross-Platform Assessment of Separation Efficiency in Ion Mobility Spectrometry. *Anal. Chem.* **2017**, *89*, 12176−12184.
(8) Borsdorf, H.; Eiceman, G. A. Ion Mobility Spectrometry: Principles and Applications. *Appl. Spectrosc. Rev.* **2006**, *41*, 323−375.
(9) Naylor, C. N.; Clowers, B. H. Reevaluating the Role of Polarizability in Ion Mobility Spectrometry. *J. Am. Soc. Mass Spectrom.* **2021**, *32*, 618−627.
(10) Shirts, R. B., Collision Theory and Reaction Dynamics. In *Gaseous Ion Chemistry and Mass Spectrometry*; Futrell, J. H., Ed.; John Wiley & Sons: New York, 1986; pp 25−57.
(11) Wyttenbach, T.; Bleiholder, C.; Bowers, M. T. Factors Contributing to the Collision Cross Section of Polyatomic Ions in the Kilodalton to Gigadalton Range: Application to Ion Mobility Measurements. *Anal. Chem.* **2013**, *85*, 2191−2199.
(12) Shrivastav, V.; Nahin, M.; Hogan, C. J.; Larriba-Andaluz, C. Benchmark Comparison for a Multi-Processing Ion Mobility Calculator in the Free Molecular Regime. *J. Am. Soc. Mass Spectrom.* **2017**, *28*, 1540−1551.
(13) Yang, F.; Voelkel, J. E.; Dearden, D. V. Collision Cross Sectional Areas from Analysis of Fourier Transform Ion Cyclotron Resonance Line Width: A New Method for Characterizing Molecular Structure. *Anal. Chem.* **2012**, *84*, 4851−4857.
(14) Anupriya; Jones, C. A.; Dearden, D. V. Collision Cross Sections for 20 Protonated Amino Acids: Fourier Transform Ion Cyclotron Resonance and Ion Mobility Results. *J. Am. Soc. Mass Spectrom.* **2016**, *27*, 1366−1375.
(15) Anupriya; Gustafson, E.; Mortensen, D. N.; Dearden, D. V. Quantitative Collision Cross-sections from FTICR Linewidth Measurments: Improvements in Theory and Experiment. *J. Am. Soc. Mass Spectrom.* **2018**, *29*, 251−259.
(16) Mao, L.; Chen, Y.; Xin, Y.; Zheng, L.; Kaiser, N. K.; Marshall, A. G.; Xu, W. Collision Cross Section Measurements for Biomolecules within a High-Resolution Fourier Transform Ion Cyclotron Resonance Cell. *Anal. Chem.* **2015**, *87*, 4072−4075.
(17) Jiang, T.; Chen, Y.; Mao, L.; Marshall, A. G.; Xu, W. Extracting biomolecule collision cross sections from high-resolution FT-ICR mass spectral linewidths. *Phys. Chem. Chem. Phys.* **2016**, *18*, 713−717.
(18) Li, D.; Tang, Y.; Xu, W. Ion collision cross section measurements in Fourier transform-based mass analyzers. *Analyst* **2016**, *141*, 3554−3561.
(19) Sanders, J. D.; Grinfeld, D.; Aizikov, K.; Makarov, A.; Holden, D. D.; Brodbelt, J. S. Determination of Collision Cross-Sections of Protein Ions in an Orbitrap Mass Analyzer. *Anal. Chem.* **2018**, *90*, 5896−5902.
(20) Dziekonski, E. T.; Johnson, J. T.; Lee, K. W.; McLuckey, S. A., CRAFTIEST: Cross Sectional Areas by Fourier Transform in Electrostatic Traps. In *65th ASMS Conference on Mass Spectrometry and Allied Topics*; American Society for Mass Spectrometry: Indianapolis, IN, 2017.
(21) Dziekonski, E. T.; Johnson, J. T.; Lee, K. W.; McLuckey, S. A. Determination of Collision Cross Sections Using a Fourier Transform Electrostatic Linear Ion Trap Mass Spectrometer. *J. Am. Soc. Mass Spectrom.* **2018**, *29*, 242−250.
(22) Elliott, A. G.; Harper, C. C.; Lin, H. W.; Susa, A. C.; Xia, Z. J.; Williams, E. R. Simultaneous Measurements of Mass and Collisional Cross-Section of Single Ions with Charge Detection Mass Spectrometry. *Anal. Chem.* **2017**, *89*, 7701−7708.
(23) Heravi, T.; Shen, J.; Johnson, S.; Asplund, M. C.; Dearden, D. V. Halide Size-Selective Binding by Cucurbit[5]uril—Alkali Cation Complexes in the Gas Phase. *J. Phys. Chem. A* **2021**, *125*, 7803.
(24) Dearden, D. V.; Liang, Y.; Nicoll, J. B.; Kellersberger, K. A. Study of Gas Phase Molecular Recognition Using Fourier Transform Ion Cyclotron Resonance Mass Spectrometry (FTICR/MS). *J. Mass Spectrom.* **2001**, *36*, 989−997.
(25) Chiavarino, B.; Crestoni, M. E.; Fornarini, S. Gas-Phase Reactivity of Organosilane Radical Cations. An FT-ICR Study. *Organometallics* **2000**, *19*, 844−848.
(26) Jones, C. A.; Dearden, D. V. Linewidth Pressure Measurement: a New Technique for High Vacuum Characterization. *J. Am. Soc. Mass Spectrom.* **2015**, *26*, 323−329.
(27) Blakney, G. T.; Hendrickson, C. L.; Marshall, A. G. Predator data station: A fast data acquisition system for advanced FT-ICR MS experiments. *Int. J. Mass Spectrom.* **2011**, *306*, 246−252.
(28) Caravatti, P.; Allemann, M. The 'Infinity Cell': a New Trapped-ion Cell With Radiofrequency Covered Trapping Electrodes for Fourier Transform Ion Cyclotron Resonance Mass Spectrometry. *Org. Mass Spectrom.* **1991**, *26*, 514−518.
(29) Sievers, H. L.; Grützmacher, H.-F.; Caravatti, P. The geometrical factor of infinitely long cylindrical ICR cells for collision energy-resolved mass spectrometry: appearance energies of EI_2^+ (E = P, As, Sb, and Bi) from collision-induced dissociation of EI_3^+ and $[EI{\bullet}ligand]^+$ complexes. *Int. J. Mass Spectrom. Ion Processes* **1996**, *157/158*, 233−247.
(30) Wigger, M.; Nawrocki, J. P.; Watson, C. H.; Eyler, J. R.; Benner, S. A. Assessing Enzyme Substrate Specificity Using Combinatorial Libraries and Electrospray Ionization-Fourier Transform Ion Cyclotron Resonance Mass Spectrometry. *Rapid Commun. Mass Spectrom.* **1997**, *11*, 1749−1752.
(31) Chen, L.; Wang, T.-C. L.; Ricca, T. L.; Marshall, A. G. Phase-Modulated Stored Waveform Inverse Fourier Transform Excitation for Trapped Ion Mass Spectrometry. *Anal. Chem.* **1987**, *59*, 449−454.
(32) Jiao, C. Q.; Ranatunga, D. R. A.; Vaughn, W. E.; Freiser, B. S. A Pulsed-Leak Valve for Use with Ion Trapping Mass Spectrometers. *J. Am. Soc. Mass Spectrom.* **1996**, *7*, 118−122.
(33) Phelps, A. V. Cross Sections and Swarm Coefficients for Nitrogen Ions and Neutrals in N_2 and Argon Ions and Neutrals in Ar for Energies from 0.1 eV to 10 keV. *J. Phys. Chem. Ref. Data* **1991**, *20*, 557−573.
(34) Marshall, A. G.; Hendrickson, C. L.; Jackson, G. S. Fourier Transform Ion Cyclotron Resonance Mass Spectrometry: A Primer. *Mass Spectrom. Rev.* **1998**, *17*, 1−35.
(35) Halgren, T. A. Merck molecular force field. I. Basis, form, scope, parameterization, and performance of MMFF94. *J. Comput. Chem.* **1996**, *17*, 490−519.
(36) Halgren, T. A. Merck molecular force field. II. MMFF94 van der Waals and electrostatic parameters for intermolecular interactions. *J. Comput. Chem.* **1996**, *17*, 520−552.
(37) Halgren, T. A. Merck molecular force field. III. Molecular geometries and vibrational frequencies for MMFF94. *J. Comput. Chem.* **1996**, *17*, 553−586.
(38) Halgren, T. A. Merck molecular force field. IV. conformational energies and geometries for MMFF94. *J. Comput. Chem.* **1996**, *17*, 587−615.
(39) Halgren, T. A. Merck molecular force field. V. Extension of MMFF94 using experimental data, additional computational data, and empirical rules. *J. Comput. Chem.* **1996**, *17*, 616−641.

https://doi.org/10.1021/jasms.1c00297
J. Am. Soc. Mass Spectrom. 2022, 33, 131−140

(40) Yang, F.; Jones, C. A.; Dearden, D. V. Effects of Kinetic Energy and Collision Gas on Measurement of Cross Sections by Fourier Transform Ion Cyclotron Resonance Mass Spectrometry. *Int. J. Mass Spectrom.* **2015**, *378*, 143−150.
(41) May, J. C.; Goodwin, C. R.; Lareau, N. M.; Leaptrot, K. L.; Morris, C. B.; Kurulugama, R. T.; Mordehai, A.; Klein, C.; Barry, W.; Darland, E.; Overney, G.; Imatani, K.; Stafford, G. C.; Fjeldsted, J. C.; McLean, J. A. Conformational Ordering of Biomolecules in the Gas Phase: Nitrogen Collision Cross Sections Measured on a Prototype High Resolution Drift Tube Ion Mobility-Mass Spectrometer. *Anal. Chem.* **2014**, *86*, 2107−2116.
(42) Lehn, J.-M. Cryptates: The Chemistry of Macropolycyclic Inclusion Complexes. *Acc. Chem. Res.* **1978**, *11*, 49−57.
(43) Gokel, G. W. *Crown Ethers and Cryptands*; Royal Society of Chemistry: Cambridge, UK, 1991.
(44) Guo, D.; Xin, Y.; Li, D.; Xu, W. Collision cross section measurements for biomolecules within a high-resolution FT-ICR cell: theory. *Phys. Chem. Chem. Phys.* **2015**, *17*, 9060−9067.
(45) Tang, Y.; Li, D.; Cao, D.; Xu, W. Extracting biomolecule collision cross sections from FT-ICR mass spectral line shape. *Talanta* **2019**, *205*, 120093.

https://doi.org/10.1021/jasms.1c00297
J. Am. Soc. Mass Spectrom. 2022, 33, 131−140